

1 **Using $^{210}\text{Pb}_{\text{ex}}$ measurements to quantify soil redistribution along two complex**
2 **toposequences in Mediterranean agroecosystems, northern Spain**

3
4 Gaspar, L.^{1,2*}, Navas, A.², Machín, J.², Walling, D.E.³

5
6 ¹ Cranfield University, Cranfield Water Sciences Institute, Cranfield, Bedfordshire
7 MK43 0AL, United Kingdom.

8 ² Department of Soil and Water, Estación Experimental de Aula Dei, EEAD-CSIC.
9 Avda Montañana 1005, 50059 Zaragoza, Spain.

10 ³ Department of Geography, College of Life and Environmental Sciences, University of
11 Exeter. Amory Building, Rennes Drive, Exeter EX4 4RJ, United Kingdom.

12
13 *Corresponding author. E-mail, leticia.gaspar.ferrer@gmail.com, l.gasparferrer@cranfield.ac.uk,
14

15 **Abstract**

16 Information on soil redistribution rates associated with the intricate patterns of
17 Mediterranean agroecosystems is a key requirement for assessing both soil degradation,
18 and off-site sediment problems that can affect downstream water bodies. Excess lead-
19 $^{210}\text{Pb}_{\text{ex}}$ measurements provide a very effective means of documenting spatial
20 patterns of rates of soil redistribution in different landscapes, but to date the approach
21 has not been widely used in mountain Mediterranean landscapes. This research aims to
22 use $^{210}\text{Pb}_{\text{ex}}$ measurements to estimate soil redistribution rates on slopes uncultivated and
23 under cultivation, within two complex toposequences located in the vicinity of Estaña
24 Lake, characterized by an intricate mosaic of land use, steep slopes and anthropogenic
25 modification (e.g. terraces and tracks), which are typical of these agroecosystems in

26 northeastern Spain. A perceptual model is developed to account for the soil
27 redistribution dynamics along both toposequences. This provides a simple and novel
28 methodology adapted to Mediterranean agroecosystems, which besides using
29 information on soil redistribution rates provided by $^{210}\text{Pb}_{\text{ex}}$ measurements, also takes
30 into account variations in land use and the presence of linear landscape elements, which
31 modify runoff and soil redistribution processes and sediment connectivity along the
32 toposequences. The results show that erosion predominated on the steep cultivated
33 slopes, but lower soil redistribution rates were found on the uncultivated slopes. On the
34 flat areas at the bottom of both transects, deposition was dominant. Variations in land
35 use and the presence of linear landscape elements control soil redistribution processes.
36 Such elements can perform the role of Ecological Focus Areas (EFAs), proposed within
37 'The Green' Common Agricultural Policy for 2014, in which at least 7 % of a farmer's
38 land should comprise EFAs, which can include terraces, landscape features, buffer strips
39 and afforested areas.

40

41 **Keywords:** $^{210}\text{Pb}_{\text{ex}}$; Soil erosion; Soil redistribution rates; land use; CAP; linear
42 landscape elements; Mediterranean agroecosystems.

43

44 **1 Introduction**

45 Soil degradation by water erosion represents one of the major environmental problems
46 facing the sustainable management of soil and soil productivity. Cultivation is seen as a
47 key factor promoting soil mobilization and soil loss. Other related effects, including the
48 mobilization and transport of sediment-associated contaminants (pesticides, fertilizers)
49 and the siltation of wetland areas must also be taken into account to protect fragile
50 agroecosystems. In addition, soil erosion transfers soil organic carbon from topsoil to

51 deposition sinks in the landscape and promotes soil carbon replacement at eroded sites
52 (Ritchie and McCarty, 2003).

53 Increased awareness of the problems of soil loss in the last decade has promoted actions
54 to conserve soil under the European Common Agricultural Policy (CAP), including the
55 most recent Green Areas initiative. In Mediterranean mountain agroecosystems large
56 areas of agricultural land were abandoned during the past century as a result of major
57 socio-economic changes. In recent years, however, some steep marginal lands have
58 been returned to cultivation under the European Agrarian Policy (García-Ruiz et al.,
59 2008; García-Ruiz, 2010; Gaspar et al., 2013). The study area selected for this research
60 is a good example of mountain areas in northern Spain, which illustrates many of the
61 problems associated with steep slopes, high rainfall intensity, changes of land use, and
62 especially the abandonment of the less productive land located on steep slopes. Previous
63 studies highlight the importance of soil erosion in the study area, especially in cultivated
64 areas. For cropland areas, Navas et al. (2012a) used caesium-137 (^{137}Cs) measurements
65 to estimate erosion rates as high as $108 \text{ Mg ha}^{-1} \text{ year}^{-1}$, while López-Vicente and Navas
66 (2010) predicted severe erosion rates ($> 100 \text{ Mg ha}^{-1} \text{ year}^{-1}$), using a combination of the
67 RMMD and SED models, in gullies on Keuper facies. In the study area, the term
68 ‘uncultivated’ has been used to refer to a range of conditions including areas of
69 undisturbed natural vegetation and areas under Mediterranean forest and scrub, as well
70 as old abandoned fields in long-term fallow (> 100 years), which are now covered by
71 dense scrub, and the more recently abandoned fields (ca. 50 years) that have a much
72 reduced vegetation cover. This leads to the development of a spatial pattern of vegetated
73 patches and bare cultivated inter-patch areas, affecting water redistribution and it is well
74 established that vegetation development and vegetation structure affect the connectivity
75 of runoff and soil redistribution processes on slopes (Cerdá 1997).

76 Lead-210 (^{210}Pb) is a natural geogenic radioisotope (half life, 22.2 yr) of the uranium
77 decay series. Decay of radium-226 in the soil and regolith releases radon-222 (^{222}Rn),
78 which in turn decays to ^{210}Pb . Some of the ^{222}Rn diffuses upward through the soil and
79 enters the atmosphere where it decays to ^{210}Pb and is returned to the earth's surface as
80 fallout. Fallout ^{210}Pb reaching the soil surface is rapidly adsorbed by clay minerals and
81 organic matter, and its subsequent redistribution is controlled by soil redistribution
82 processes in a manner similar to ^{137}Cs (Walling and He, 1999a, b). This fallout ^{210}Pb is
83 termed unsupported or excess ^{210}Pb ($^{210}\text{Pb}_{\text{ex}}$), since it is not in equilibrium with its
84 parent ^{226}Ra . $^{210}\text{Pb}_{\text{ex}}$, like ^{137}Cs , offers the potential for use as a tracer in estimating rates
85 of soil redistribution. However, $^{210}\text{Pb}_{\text{ex}}$ measurements have been less widely used for
86 estimating soil redistribution rates than ^{137}Cs , although their use has increased
87 significantly in recent years (e.g. Wallbrink and Murray, 1993; Walling and Quine,
88 1995; He, Q. and Walling, D.E. 1996; Zhang, et al., 2006; Kato et al., 2010; Porto and
89 Walling, 2012; Benmansour et al., 2013).

90 The continuous input of $^{210}\text{Pb}_{\text{ex}}$ fallout through time means that the contemporary
91 $^{210}\text{Pb}_{\text{ex}}$ inventory in the soil will reflect soil redistribution and thus loss and gain of
92 $^{210}\text{Pb}_{\text{ex}}$ occurring within a period equivalent to four times the half-life, and thus the past
93 100 years (Walling et al., 2003). However, the effect of past changes in the $^{210}\text{Pb}_{\text{ex}}$
94 inventory, caused by erosion and deposition, on the contemporary inventory, will
95 progressively decline as the period of time elapsed increases and this must be taken into
96 account when interpreting the impact of the erosional history of a study site on the
97 magnitude of the contemporary $^{210}\text{Pb}_{\text{ex}}$ inventory. This inventory will clearly be more
98 sensitive to recent soil redistribution, and the estimate of the mean rate of soil
99 redistribution for the past ca. 100 years provided by the conversion model used to
100 estimate the soil redistribution rate from a comparison of the inventory measured at a

101 sampling point with the local reference inventory is likely to be biased towards the
102 recent erosional history of the study site.

103 In order to understand soil redistribution dynamics in the intricate toposequences that
104 are characteristic of the typical agroecosystems of northern Spain, it is important to
105 know how the interfacing of patches of different land use and linear landscape elements
106 modify soil redistribution processes and the sediment connectivity along the slopes. The
107 use of $^{210}\text{Pb}_{\text{ex}}$ measurements provides a means of investigating such systems. Their use
108 to investigate both cultivated and uncultivated soils and to quantify sediment sources
109 and sinks along slopes of different aspect represents a novel application, particularly
110 within a mountain agricultural area. The use of $^{210}\text{Pb}_{\text{ex}}$ measurements to document soil
111 redistribution rates and analysis of the factors that affect soil redistribution along
112 toposequences of different aspect affords a means of developing an improved
113 understanding of the role of land use, soil type and slope gradient in Mediterranean
114 agroecosystems. Additionally, the development of a perceptual model of soil movement
115 of redistribution rates, which take into account changes in land uses and the presence of
116 linear landscape elements, is seen as potentially offering a new tool to elucidate
117 sediment connectivity in intricate landscapes. This is of importance for developing
118 'green' agricultural practices, as 'The Green' CAP proposes that at least 7 % of farmland
119 should be converted to Ecological Focus Areas.

120 The objectives of this study were therefore to use $^{210}\text{Pb}_{\text{ex}}$ measurements to estimate the
121 long-term mean annual rate of soil redistribution on cultivated and uncultivated soils
122 along two slope transects representatives of Mediterranean agroecosystems in NE of
123 Spain. Its results aim to contribute to a better understanding of the impact of land use
124 and the presence of linear landscape elements (both natural features and anthropogenic
125 infrastructure) on soil redistribution processes along toposequences. Additionally,

126 assessment of the importance of natural features for trapping and storing eroded soil, as
127 promoted by the new Common Agricultural Policy (CAP) is a key requirement for both
128 the sustainable management of the soil resource and the protection of downstream
129 aquatic ecosystems from degradation resulting from increased sediment loads. Finally,
130 the development of a perceptual model of soil movement aims to elucidate how linear
131 landscape elements contribute to patterns of soil redistribution along cultivated and
132 uncultivated toposequences.

133

134 **2 Material and methods**

135 *2.1 Study area*

136 The study was conducted along two representative toposequences located in the Spanish
137 central Pre-Pyrenees (NE Spain), close to the northern boundary of the Ebro river basin
138 (Figure 1). This area includes a freshwater lake. Estaña Lake, in the lower part of the
139 landscape that has been under regional protection since 1997 and is included in the
140 European NATURA 2000 network as a Site of Community Importance. The average
141 annual precipitation is 595 mm (1997-2006) with two wet periods, spring and autumn,
142 and a dry summer with high intensity rainfall events extending from July to October.
143 The average annual temperature is 12.2° C, with thermal inversions common during the
144 winter (López-Vicente et al., 2008). The Mediterranean agroecosystem of the study area
145 comprises an intricate landscape, characterized by abrupt relief with slope gradients up
146 to 34 %. The cultivated and uncultivated areas are heterogeneously distributed. The
147 cultivated fields are located in the lower and mid slope areas and are separated by
148 vegetation strips, while uncultivated areas predominate on the steep slopes. Winter
149 barley is the main crop and, as indicated above, uncultivated areas include areas of
150 Mediterranean forest, scrubland and abandoned fields recolonised by natural vegetation.

151 The predominant soil types along the toposequences are stony Calcisols and Regosols.
152 Leptosols are restricted to the upper part of the slope under Mediterranean forest
153 underlain by Muschelkalk facies, and Gypsisols cultivated for cereals are restricted to
154 the lower part of one of the transects underlain by Keuper facies.

155 Two representative hillslope transects, extending from the divide to the lake, were
156 selected to represent different toposequences within this agroecosystem (Figure 1). A
157 total of 34 sampling sites, approximately 50 m apart were established along both
158 transects. However, it was recognised that tillage erosion in fields delimited by furrows
159 and tracks can cause significant soil redistribution both at the head and the bottom of the
160 fields (Gaspar, 2011), and thus the spacing of the sampling sites on the lower cultivated
161 part of the ST was reduced to 25 m, in order to provide a reliable representation of soil
162 redistribution in this area (Figure 1).

163 The northern transect NT (S-N) is 300 m long and characterized by a 10 % slope. Its
164 altitude ranges from 711 to 682 m and the seven sampling sites are located on a gentle
165 north facing slope occupied exclusively by uncultivated areas. Regosols are restricted to
166 the upper part of the transect while Calcisols predominated in the rest of the transect.

167 The southern transect ST (N-S) is 1110 m long and extends down a steeper south facing
168 slope (21 % slope) with an altitude ranges from 894 to 676 m. The transect crosses
169 patches of different land use. The uncultivated areas are located primarily on the upper
170 and midslope sections of the transect on Calcisols and Regosols, whereas the cultivated
171 fields are located on the midslope on stony Calcisols and Regosols and on the bottom
172 slope on Gypsisols with a low stone content. Leptosols are found within the upper part
173 of the transect under Mediterranean forest and on a thick Muschelkalk outcrop on the
174 midslope. ST includes 27 sampling sites and is characterized by a rugged topography
175 and the presence of agricultural terraces, a thick Muschelkalk outcrop on the midslope

176 and vegetation strips, which have an important effect on hydrological processes as they
177 reduce the local slope gradient, intercept runoff and trap eroded sediment.

178 Nine bulk cores were collected from sampling points located on cultivated soils and 24
179 sectioned profiles were collected from the sampling points on uncultivated soils, which
180 were also the subject of another study investigating the depth distribution of
181 unsupported ^{210}Pb (Gaspar, 2011). Sampling site ST-14 is located on a thick
182 Muschelkalk outcrop and soil samples for $^{210}\text{Pb}_{\text{ex}}$ measurements were not collected from
183 this point. The bulk cores obtained from the cultivated areas were collected using a 8.0
184 cm diameter hand-operated core sampler. The core depth always exceeded the plough
185 depth (ca. 20 cm), with a maximum of 55 cm. The sectioned profiles were collected
186 using a 10 x 10 cm steel box corer (Navas et al., 2008) at 2 cm depth intervals to a
187 maximum depth of 10 - 14 cm depth, which had been shown by previous work in the
188 study area to include the complete $^{210}\text{Pb}_{\text{ex}}$ profile in uncultivated soil (Gaspar, 2011). At
189 each uncultivated sampling site, a three-sided frame was driven into the ground with the
190 open end of the sampling frame facing downslope. The soil downslope of the sampler
191 was carefully removed until a block of soil was enclosed within the sample frame. A
192 blade was inserted into a series of grooves spaced at 2 cm on the sides of the device to
193 section the profiles.

194 The samples collected from each sampling point along the transects were dried, gently
195 disaggregated and sieved to < 2mm. The stone content (%) was determined as the
196 proportion > 2mm. The < 2mm fraction was analysed to obtain the total $^{210}\text{Pb}_{\text{ex}}$
197 inventory (Bq m^{-2}), the soil organic carbon (SOC) content, and the mean clay, silt and
198 sand content. The SOC content was determined by the dry combustion method using a
199 LECO RC-612 multiphase carbon analyzer. In this case, a sub-sample of the < 2 mm
200 fraction is inserted into a quartz tube, heated to 550 °C and the SOC is oxidized to CO_2 ,

201 which is selectively detected by an infrared (IR) gas analyser. Grain size analysis of the
202 < 2mm fraction to determine the sand, silt and clay content (%) was undertaken using a
203 laser granulometer. Prior to grain size analysis, organic matter was removed from the
204 samples using 10% H₂O₂ heated to 80 °C and the mineral sediment was ultrasonically
205 dispersed.

206

207 2.2 Using ²¹⁰Pb_{ex} as a sediment tracer

208 To determine the ²¹⁰Pb_{ex} inventory at each sampling point, a representative aliquot of
209 the < 2mm fraction of the bulk core or the individual sections of the sectioned cores was
210 placed into a cylindrical plastic container and sealed for 40 days prior to assay in order
211 to achieve equilibrium between ²²⁶Ra and its daughter ²¹⁴Pb. The ²¹⁰Pb_{ex} activity in the
212 sample was measured by gamma-ray spectrometry, using a high resolution low energy
213 coaxial HPGe detector coupled to an amplifier (broad energy detector (BeGe)). The
214 detector had an efficiency of 30 % and a resolution of 1.9 keV, and was contained
215 within a lead shield to reduce the background. Calibration was achieved using standard
216 certified samples with the same geometry and bulk density as the measured samples.
217 Count time was typically ca. 86,400 s, providing results with an analytical precision of
218 ca. 10 - 15 % at the 95 % level of confidence. The total ²¹⁰Pb activity in the samples was
219 measured at 46.5 keV, and the ²²⁶Ra activity was obtained by measuring the activity of
220 ²¹⁴Pb, a short-lived daughter of ²²⁶Ra at 351.9 keV. The detection limits in Bq kg⁻¹ for
221 ²¹⁰Pb and ²¹⁴Pb were 7.45 and 1.26 Bq kg⁻¹, respectively. The ²¹⁰Pb_{ex} activity was
222 determined by subtracting the ²²⁶Ra activity from the total ²¹⁰Pb activity. The ²¹⁰Pb_{ex}
223 inventories for individual sampling points were calculated using the measured ²¹⁰Pb_{ex}
224 activities. With the sectioned cores this involved summing the values for the individual
225 sections.

226 Estimates of soil redistribution rates are derived from $^{210}\text{Pb}_{\text{ex}}$ measurements by
 227 comparing the total inventory for an individual sampling soil with the local reference
 228 inventory for the study area and using a conversion model to estimate the erosion rate
 229 represented by a reduced inventory or the deposition rate represented by an increased
 230 inventory. In order to establish the $^{210}\text{Pb}_{\text{ex}}$ reference inventory, two sectioned profiles
 231 and seven bulk cores were collected from an undisturbed location adjacent to the
 232 sampled transects, with minimal slope and no evidence of erosion or deposition, such
 233 that no sediment redistribution was likely to have occurred over the past 100 years. The
 234 undisturbed nature of the reference sites was confirmed by the $^{210}\text{Pb}_{\text{ex}}$ depth profiles that
 235 provided a well-defined exponential depth distribution. Estimates of soil redistribution
 236 rates along the two transects investigated were obtained using the conversions models
 237 for cultivated and uncultivated soils described by Walling and He (1999a) and Walling
 238 et al. (2011).

239 Soil redistribution rates on cultivated soils were estimated using a mass balance model
 240 (mass balance model 2) developed at the University of Exeter (see Walling and He,
 241 1999a). The model takes into account the continuous atmospheric deposition of $^{210}\text{Pb}_{\text{ex}}$
 242 and its subsequent decay and its redistribution in association with soil erosion and
 243 deposition. In addition, the model considers the effect of particle size selectivity of
 244 sediment mobilization, and the transport and the removal of freshly deposited fallout
 245 $^{210}\text{Pb}_{\text{ex}}$ by erosion, before its incorporation into the tillage horizon. The basic form to
 246 estimate the erosion rate R ($\text{kg m}^{-2} \text{ year}^{-1}$) can be expressed as Equation 1:

$$247 \quad \frac{dA(t)}{dt} = (1 - \Gamma)I(t) - \left(\lambda + P \frac{R}{d} \right) A(t) \quad (1)$$

248 where $A(t)$ is the cumulative $^{210}\text{Pb}_{\text{ex}}$ inventory (Bq m^{-2}); d the tillage depth (kg m -
 249 2); λ is the ^{210}Pb decay constant (year^{-1}); $I(t)$ the annual fallout $^{210}\text{Pb}_{\text{ex}}$ deposition
 250 flux at time t ($\text{Bq m}^{-2} \text{ year}^{-1}$); Γ the proportion of the freshly deposited $^{210}\text{Pb}_{\text{ex}}$

251 fallout input removed by water erosion before incorporation into the tillage layer;
 252 and P the particle size correction factor to take account of differences between the
 253 grain size composition of the mobilised sediment and the original soil (Walling and
 254 He, 1999a; Walling et al., 2003). The model used to estimate the deposition rate R'
 255 ($\text{kg m}^{-2} \text{ year}^{-1}$) takes the form indicated by Equation 2:

$$256 \quad A_{c,ex} = \int_{t_0}^t R' C_d(t') e^{-\lambda(t-t')} dt' \quad (2)$$

257 where $A_{c,ex}$ is the $^{210}\text{Pb}_{\text{ex}}$ inventory (Bq m^{-2}) and $C_d(t')$ represents the concentration
 258 of $^{210}\text{Pb}_{\text{ex}}$ in deposited sediment (Bq kg^{-1}). $C_d(t')$ can be estimated as the weighted
 259 mean $^{210}\text{Pb}_{\text{ex}}$ activity of the sediment eroded from the upslope contributing area.

260 A modified version of the diffusion and migration conversion model developed for
 261 ^{137}Cs measurements (Walling and He, 1999b) was used to estimate soil redistribution
 262 rates from $^{210}\text{Pb}_{\text{ex}}$ inventories at the uncultivated sampling points. This model assumes a
 263 constant fallout of $^{210}\text{Pb}_{\text{ex}}$ and takes into account post-depositional redistribution
 264 processes and their influence on the $^{210}\text{Pb}_{\text{ex}}$ depth distribution (Walling et al., 2011).

265 A diffusion coefficient D ($\text{kg}^2 \text{ m}^{-4} \text{ year}^{-1}$) is used to represent the net effect of the slow
 266 vertical redistribution of $^{210}\text{Pb}_{\text{ex}}$ by physicochemical and biological processes. The rate
 267 of soil loss R ($\text{kg m}^{-2} \text{ year}^{-1}$) can be estimated from the reduction of the $^{210}\text{Pb}_{\text{ex}}$ inventory
 268 at the sampling point, relative to the reference inventory for the study site ($A_{u,ls}(t)$) and a
 269 model-derived estimate of the $^{210}\text{Pb}_{\text{ex}}$ content of the surface soil ($C_u(t')$), as indicated by
 270 Equation 3:

$$271 \quad \int_0^t PRC_u(t') e^{-\lambda(t-t')} dt' = A_{u,ls}(t) \quad (3)$$

272 The deposition rates R' ($\text{kg m}^{-2} \text{ year}^{-1}$) can be estimated (Equation 4) from the increase
 273 in the $^{210}\text{Pb}_{\text{ex}}$ inventory compared with the local reference value ($A_{u,ex}(t)$), and the $^{210}\text{Pb}_{\text{ex}}$
 274 content of deposited sediment soil ($C_d(t')$) (Walling et al., 2011).

275
$$R' = \frac{A_{u,ex}}{\int_0^t C_d(t') e^{-\lambda(t-t')} dt'} \quad (4)$$

276 $C_d(t')$ can be estimated as the weighted mean $^{210}\text{Pb}_{ex}$ activity of the sediment
277 eroded from the upslope contributing area.

278 When applying the models to the $^{210}\text{Pb}_{ex}$ measurements obtained from the two transects,
279 values of 4 kg m⁻² and 1.0 were assumed for the relaxation depth (H) and particle size
280 correction (P) parameters, respectively, in both models and a value of 1.0 was assumed
281 for the proportion parameter (γ) in the mass balance model.

282 Once estimates of the soil redistribution rate were derived for each of the sampling
283 points, the methodology proposed by Collins et al., (2001) was applied to each
284 toposequence (NT and ST) to estimate the net soil redistribution rate associated with the
285 two transects. In addition, in order to refine and adapt this technique for application to
286 intricate Mediterranean landscapes, it is important to take account of the effects of linear
287 landscape elements. The presence of agricultural terraces, buffer strips, rock outcrops
288 and tracks can have an important effect on downslope runoff and sediment transfer as
289 they reduce the slope gradient and length, and trap the eroded soil, influencing the
290 distribution of areas of erosion and deposition along the slope.

291 Statistical analysis was performed by one-way analysis of variance (ANOVA), and the
292 means were subjected to a least-significant difference test (F test) to indicate the main
293 differences in $^{210}\text{Pb}_{ex}$ inventories and soil properties between cultivated and uncultivated
294 sites, and the differences in the soil redistribution rates estimated from the $^{210}\text{Pb}_{ex}$
295 measurements between the different land uses, soil types and slope gradient.

296

297 **3 Results and discussion**

298 *3.1 Assessment of soil redistribution rates using $^{210}\text{Pb}_{ex}$ inventories*

299 The reference $^{210}\text{Pb}_{\text{ex}}$ inventory for the study area estimated from nine sampling points
300 located on undisturbed soil with minimal slope adjacent to the study transects is 2019.8
301 $\pm 215.8 \text{ Bq m}^{-2}$. Figure 2 shows the depth distributions of $^{210}\text{Pb}_{\text{ex}}$ for a representative
302 reference soil profile in the study area. This reference inventory is very similar to that
303 reported for the area from a preliminary study reported by Gaspar et al. (2013) and is
304 within the range of $^{210}\text{Pb}_{\text{ex}}$ reference inventories reported by Sanchez-Cabeza et al.
305 (2007) for different parts of northern Spain (between 1044 and 8204 Bq m^{-2} , depending
306 on the mean annual rainfall of the study site). However, the reference inventory
307 obtained for the study area is smaller than values reported by other authors for different
308 areas of the world, for example: 5170 Bq m^{-2} in the UK (Walling and He, 1999a), 5730
309 and 12860 Bq m^{-2} in China (Zhang, et al., 2003 and Zhang, et al., 2006, respectively),
310 6310 Bq m^{-2} (Kato et al., 2010) and 19703 Bq m^{-2} (Wakiyama et al., 2010) in Japan,
311 5266 (Porto et al., 2006), 14572 Bq m^{-2} (Porto et al., 2009) and 7598 Bq m^{-2} (Porto and
312 Walling, 2012) in Italy, 34000 in Taiwan (Huh and Su, 2004), and between 3580 and
313 10060 Bq m^{-2} for different floodplain sites in England and Wales (Du and Walling,
314 2012).

315 The $^{210}\text{Pb}_{\text{ex}}$ inventories recorded along the two study transects showed significant
316 variability, reaching a maximum of 7298.2 Bq m^{-2} (Table 1). The ANOVA test
317 indicated that the $^{210}\text{Pb}_{\text{ex}}$ inventories were higher for cultivated soils than for
318 uncultivated soils, although the differences were not statistically significant. A similar
319 pattern has been previously documented in the study area for ^{137}Cs , and this trend
320 confirms the importance of land use in controlling fallout radionuclide inventories and
321 thus soil redistribution rates in the local area (Navas et al., 2012a; Gaspar et al., 2013).

322 The main soil properties analyzed showed values consistent with the characteristics of
323 Mediterranean agroecosystems. Information on stone content, SOC content and grain

324 size composition for cultivated and uncultivated soils are presented in Table 1. The SOC
325 and stone content were significantly higher in uncultivated soils. In cultivated soils the
326 maximum values of SOC did not exceed 2.3 %, confirming the impact of long-term and
327 intense agricultural use on SOC content (Navas et al., 2011). The relative magnitude of
328 the clay, silt and sand fractions varied greatly between the sampling points. However,
329 no significant difference was found between the two land uses, with silt-loam being the
330 predominant texture.

331 After isolating the land use factor, only SOC showed significant differences between
332 different soil types. For cultivated soils, higher inventories of $^{210}\text{Pb}_{\text{ex}}$ were found on
333 Gypsisols, while Calcisols showed significantly higher mean values of SOC and slightly
334 higher mean values of stone and sand content. In uncultivated areas, significantly higher
335 mean values of SOC was found on Leptosols, which in turn have slightly higher values
336 of $^{210}\text{Pb}_{\text{ex}}$ inventory and stone content (Table 2).

337 For the northern transect (NT), the lack of significant reduction or increase in inventory
338 values for the sampling points indicates that these points have not experienced
339 significant soil redistribution over the past 100 years, and particularly in recent years. In
340 contrast, significant increases and reductions in inventory values, relative to the
341 reference inventory, for the sampling points on the southern transect (ST), particularly
342 for cultivated points, suggest that these points have experienced appreciable soil loss or
343 deposition over that period, and indicate that significant soil redistribution has occurred
344 along transect ST, in marked contrast with the NT transect.

345 The soil redistribution rates ($\text{Mg ha}^{-1} \text{ year}^{-1}$), derived from the $^{210}\text{Pb}_{\text{ex}}$ inventories using
346 the models described above and shown in Figure 3, indicate that erosion rates range
347 between 0.1 and 83.7 $\text{Mg ha}^{-1} \text{ year}^{-1}$ and sedimentation rates range between 0.08 and
348 74.8 $\text{Mg ha}^{-1} \text{ year}^{-1}$. The highest values were found on cultivated soils, whereas on

349 uncultivated soils, erosion and deposition rates did not exceed 2.4 and 5.6 Mg ha⁻¹
350 year⁻¹, respectively (Table 3). As shown in Figure 3, the soil redistribution rates follow
351 quite closely the changes in land use. For the uncultivated transect (NT) most sampling
352 points recorded low erosion rates, with a maximum of 2.4 Mg ha⁻¹ year⁻¹ (NT-6) and
353 most values close to stability (NT-1, NT-4, NT-5). The highest sedimentation rates were
354 found at the bottom part of the transect (NT-7) and did not exceed 5.6 Mg ha⁻¹ year⁻¹.
355 On the contrary, the combined effects of topography and tillage have caused different
356 patterns of soil redistribution along the ST. Uncultivated areas on ST evidence similar
357 soil redistribution rates to those found on NT and soil stability predominates. In the
358 upper part of ST the dense forest protected the soil surface from erosion (ST-1, ST-3)
359 and higher deposition rates, that did not exceed 1.3 Mg ha⁻¹ year⁻¹ (ST-20), were
360 identified on the relatively flat areas (ST-6, ST-10, ST-17). The highest erosion rate
361 within the uncultivated areas was located at ST-19 (2.3 Mg ha⁻¹ year⁻¹), which
362 corresponds to open scrubland. On the steeper cultivated slopes, sampling points ST-13,
363 ST-15 and ST-16 recorded high erosion rates (between 5.4 and 54.20 Mg ha⁻¹ year⁻¹).
364 In contrast, on cultivated flat areas at the bottom part of the ST, sampling points ST-23,
365 ST-24, ST-26 and ST-27 evidenced the highest deposition rates, but the highest erosion
366 rate was also found at ST-25 (83.7 Mg ha⁻¹ year⁻¹). Previous research in this area with
367 ¹³⁷Cs and ²¹⁰Pb_{ex} (Gaspar et al., 2013) provide evidence that tillage erosion was
368 important in these cultivated fields. The soil redistribution rates estimated from the
369 ²¹⁰Pb_{ex} measurements are in agreement with those obtained from ¹³⁷Cs measurements in
370 the same study area, using appropriate conversion models (Soto and Navas, 2004,
371 2008), which ranged between 2.6 and 31.9 Mg ha⁻¹ year⁻¹ for erosion rates, and
372 between 0.2 and 24.5 Mg ha⁻¹ year⁻¹ for deposition rates. These results demonstrate the
373 important effect of agricultural activities on soil redistribution. The presence of ridges

374 and furrows causes a local increase in slope gradient on the side of the furrow, relative
375 to the natural slope, which will increase rates of interrill erosion (Junge et al., 2010).

376 The mean erosion rates for the cultivated fields were significantly higher than for the
377 uncultivated areas. Slightly higher erosion rates were found on Regosols than on
378 Leptosols and Calcisols, although differences were not significant, while on Gypsisols
379 the mean erosion rates were significantly higher. Table 4 indicates that erosion rates
380 were similar in areas with average slope between 0 to 12 % and 12 to 24 % and that
381 these rates appeared to be higher than those on steeper slopes (> 24 %), although the
382 difference was not statistically significant. The mean deposition rates were significantly
383 higher for cultivated areas and on Gypsisols. However, unlike the erosion rates,
384 significantly higher deposition rates were found on flat areas (0 to 12 %) (Table 4).

385 In the study area, land use, soil type and slope gradient are linked. Most of the
386 uncultivated profiles were on Leptosols and Calcisols, located along the upper part of
387 ST and along NT and these points had the lowest rates of soil redistribution. While,
388 most cultivated sampling points were on Gypsisols, these were located on the flatter
389 lower part of ST, which recorded the highest redistribution rates (both erosion and
390 deposition). On Regosols, the cultivated sampling points were on steep slopes, while the
391 sampling points on uncultivated areas consisted of open scrubland. Both favoured
392 redistribution processes.

393 Principal components loadings and biplot after varimax rotation (Table 5, Figure 4) show
394 that for erosion rates, three components were retained with eigenvalues higher than one,
395 explaining 74 % of total variance. The first principal component, which represents 32 % of
396 the total of variance, showed high values for the variables related to grain size. The second
397 component, with 29 % of total variance, showed high loading values of the parameters
398 related to land use and erosion rates, which were negatively correlated with SOC and also

399 with stone content but the estimated communality of this particular variable is lower than
400 0.5 and represents a low proportion of the variance. The third component was associated
401 with the slope factor, which was negatively correlated with SOC, and represents 13 % of
402 variance (Table 5.a). For deposition rates, two components explained 78 % of the total
403 variance. The first component, which represents 54 % of the total variance, showed high
404 loading values for the parameters related to land use and deposition rates, which were
405 negatively correlated with SOC, slope factor and stoniness, while the second component,
406 with 24 % of total variance, showed high loading values of the parameters related to grain
407 size (Table 5.b).

408 Although PCA cannot be used numerically for prediction purposes, the PCA biplot (Figure
409 4a, 4b) is of interest as it indicates the level of correlation between the analyzed variables.
410 Both erosion and deposition rates are positively correlated with land use. Likewise, the fact
411 that SOC is negatively correlated with erosion rates can be interpreted to mean that soil
412 loss is associated with loss of organic carbon (Figure 4.a), as reported for similar
413 environments by Navas et al. (2012b) and in agreement with Ritchie and McCarty
414 (2008), who also reported strong links between soil redistribution and soil organic
415 carbon concentrations in agricultural soils. In addition, the fact that stone content and
416 slope are negatively correlated with deposition rates can be interpreted to mean that in flat
417 areas evidencing a lower stone content deposition processes predominate (Figure 4.b).

418 Despite the small sample size ($n=20$ for erosion rates and $n=13$ for deposition rates), the
419 communality of most variables was higher than 0.5 (Table 5a, 5b), thus the extracted
420 components account for a substantial proportion of the variable's variance. This means that
421 these variables are reflected well via the extracted components, and hence that the PCA
422 analysis was reliable.

423

424 *3.2 A quantitative perceptual model for estimating soil redistribution rates and the*
425 *effect of linear landscape elements*

426 Assuming that each transect represents a 1 m wide strip, values of soil redistribution
427 rate obtained for each sampling point were used to calculate equivalent values of soil
428 loss or deposition (kg year^{-1}) for individual slope segments, extending halfway to the
429 adjacent coring points from the sampling point in each direction, as reported by Collins
430 et al. (2001), Walling et al. (2003) and Estrany et al. (2010). However, this methodology
431 was modified to adapt it to the characteristics of the study transects, in order to take into
432 account changes in land use and the presence of linear landscape elements. This was
433 achieved by relating the segment length to vegetation cover and introducing the linear
434 landscape elements.

435 The resulting values for each segment were summed to provide a total erosion and total
436 deposition, respectively, thus obtaining net soil loss for each transect ($\text{Mg ha}^{-1} \text{ year}^{-1}$)
437 and the sediment delivery ratio (%) (cf. Walling et al., 2003). For NT, the total erosion
438 is estimated at 26 kg year^{-1} and total deposition at $25.8 \text{ kg year}^{-1}$. The net soil loss of 0.2
439 kg year^{-1} ($0.01 \text{ Mg ha}^{-1} \text{ year}^{-1}$ and a sediment delivery ratio of 0.7 %) indicates that soil
440 redistribution processes have a limited effect on this transect. The presence of a stone
441 embankment between NT-4 and NT-5, and an unpaved trail between NT-6 and NT-7 is
442 likely to modify the runoff and sediment connectivity along the transect, except during
443 intense rainfall events. In contrast, for ST the total erosion is estimated to be 637 kg
444 year^{-1} and total deposition at 705 kg year^{-1} , representing a net soil accumulation of 68 kg
445 year^{-1} ($1.24 \text{ Mg ha}^{-1} \text{ year}^{-1}$ and a negative sediment delivery ratio), with this especially
446 concentrated along the bottom part of the ST.

447 Transect ST is characterized by the presence of a thick Muschelkalk outcrop at the
448 midslope, between ST-13 and ST-15, which disrupts the runoff and sediment

449 connectivity along the transect. In addition, an unpaved trail located on the bottom slope
450 (between ST-24 and ST-25), a system of old terraces located in the upper part of the
451 transect (between ST-10 and ST-11) and several vegetation strips (Figure 5), also
452 modify the topography and change the runoff and sediment connectivity along the
453 transect.

454 Considering the natural elements and human modifications, mentioned above, transect
455 ST was divided into seven sections (Figure 5). During normal rainfall events the linear
456 landscape elements restrict the runoff and the downslope transfer of soil previously
457 eroded within each of the seven sections. However, during intense and erosive rainfall
458 events only the thick outcrop disrupts the soil redistribution processes along ST. In the
459 upper part of the transect, the vegetation cover on uncultivated areas is dense and, in
460 spite of the presence of the steepest slopes, the first three sections recorded low values
461 of net soil loss (0.3, 0.3, 2.8 Mg ha⁻¹ year⁻¹, respectively, and sediment delivery ratios of
462 63, 100 and 100 %, respectively). In sections four and five higher values of net soil loss
463 coincide with cultivated soils on steep slope (54.2 and 12.9 Mg ha⁻¹ year⁻¹, respectively,
464 and the corresponding sediment delivery ratios were 100 %). Section six is
465 characterized by low erosion rates on uncultivated areas and net soil deposition (6.5 Mg
466 ha⁻¹ year⁻¹), which occurs in the cultivated fields above the trail. The last sections
467 correspond with cultivated flat areas below the trail, with higher net soil deposition
468 (1.91 Mg ha⁻¹ year⁻¹).

469 This methodology provides information regarding erosion and deposition rates, as well
470 as the net soil loss from the transects, and how land use and linear landscape elements
471 modify the soil redistribution processes and sediment connectivity.

472 The patterns of ²¹⁰Pb_{ex} redistribution along both NT and ST demonstrate that in
473 Mediterranean environments cultivated land exerts an important control on soil loss

474 stressing the need to encourage the participation of the farmers in soil conservation
475 programs. Furthermore, these results suggest that deposition rates associated with
476 cultivated areas are affected by the presence of flat topography and soil conservation
477 practices, while deposition rates on uncultivated areas are linked to changes from
478 convex to concave slopes, the presence of transverse terraces and vegetation buffer
479 strips, which reduce runoff velocity. These results emphasize the potential of the new
480 green areas program proposed by CAP to control soil loss in agricultural ecosystems.
481 Sediment mobilised from the upslope areas may be deposited in the Estaña lake located
482 downslope of the investigated transects. The net soil deposition rates obtained for NT
483 and ST are influenced by the location of the soil sampling sites selected along 1 m wide
484 strip. However, previous research using ^{137}Cs measurements (Gaspar et al., 2013)
485 showed high activity of ^{137}Cs in deeper layers at a sampling point situated on the margin
486 of the Estaña lake, adjacent to ST-27 at the bottom of the ST. This profile corresponds
487 to a lake sediment deposit, as indicated by the presence of the 1963 ^{137}Cs peak at a
488 depth of 45 cm, which means an accumulation sediment of $113 \text{ Mg ha}^{-1} \text{ year}^{-1}$ at this
489 point.

490

491 **4 Conclusions**

492 This study has demonstrated the potential of $^{210}\text{Pb}_{\text{ex}}$ measurements to estimate soil
493 erosion and deposition along the toposequences that are characteristic of hillslopes in
494 mountain Mediterranean agroecosystems. For intricate transects, the sampling strategy
495 should take into account changes in land use and the presence of linear elements in
496 cultivated fields that might intensify tillage erosion at the head of the fields. For
497 transects with homogeneous land use, a spacing of 50 m between sampling points is
498 considered sufficient to provide meaningful estimates of soil redistribution rates. This

499 contribution describes similar soil redistribution patterns along the toposequences to
500 those established using ^{137}Cs , $^{210}\text{Pb}_{\text{ex}}$ and prediction models in previous research.

501 The spatial variability of soil redistribution rates along the toposequences was closely
502 controlled by land use that was in turn closely related to vegetation cover, topography,
503 soil type and slope gradient. Our results show that on steep cultivated slopes erosion
504 processes predominated, whereas uncultivated areas were characterized by lower soil
505 redistribution rates. On the flat areas at the bottom of both transects, sedimentation
506 processes dominated over erosion. The marked variations of SOC content along the
507 transect clearly reflect the variety of land use along the transects and their complex
508 physiography.

509 Land use and slope gradient exert important controls on the soil redistribution rates. For
510 steep slopes on the upper part of the transects, the open Mediterranean forest and
511 scrubland protect the soil surface from erosion, while the cultivated soils are more
512 vulnerable to erosion and soil redistribution is more intense. Vegetation cover together
513 with topography and tillage are key factors affecting the pattern of soil redistribution on
514 the transects.

515 Assessing erosion and deposition rates for cultivated and uncultivated soils has proved
516 useful for understanding the dynamics of soil redistribution in mountain
517 agroecosystems. The application of a quantitative perceptual model has provided
518 information to assess the effects of linear landscape elements along complex
519 toposequences. This research has contributed information on the potential role of linear
520 landscape elements and vegetation buffer strips in controlling sediment transfer along
521 hillslopes within Mediterranean agroecosystems.

522

523 **Acknowledgements**

524 Financial support from CICYT project EROMED (CGL2011-25486/BTE) is gratefully
525 acknowledged. Financial support of the Spanish CAI social work bank for a
526 postdoctoral fellowship during 2012 is gratefully acknowledged.

527

528 **References**

529 Benmansour, M., Mabit, L., Noura, A., Moussadek, R., Bouksirate, H., Duchemin, M.,
530 Benkdad, A., 2013. Assessment of soil erosion and deposition rates in a Moroccan
531 agricultural field using fallout ^{137}Cs and $^{210}\text{Pb}_{\text{ex}}$. *J. Environ. Radioactiv.* 115, 97-106.

532 Cerdà, A., 1997. Soil erosion after land abandonment in a semiarid environment of
533 southeastern Spain. *Arid. Soil Res. Rehabil.* 11(2), 163-176.

534 Collins, A.L., Walling, D.E., Sickingabula, H.M., Leeks, G.J.L., 2001. Using ^{137}Cs
535 measurements to quantify soil erosion and redistribution rates for areas under different
536 land use in the Upper Kaleya River basin, southern Zambia. *Geoderma* 104, 299-323.

537 Du, P., Walling, D.E., 2011. Using ^{137}Cs measurements to investigate the influence of
538 erosion and soil redistribution on soil properties. *Appl. Radiat. Isot.* 69, 717-726.

539 Estrany, J., García, C., Walling, D., 2010. An investigation of soil erosion and
540 redistribution in a Mediterranean lowland agricultural catchment using caesium-137.
541 *Int. J. Sediment Res.* 25, 1-16.

542 García-Ruiz, J.M., 2010. The effects of land uses on soil erosion in Spain: A review.
543 *Catena* 81, 1-11.

544 García-Ruiz, J.M., Regües, D., Alvera, B., Lana-Renault, N., Serrano-Muela, P., Nadal-
545 Romero, E., Navas, A., Latron, J., Martí-Bono, C., Arnáez, J., 2008. Flood generation
546 and sediment transport in experimental catchments affected by land use changes in the
547 central Pyrenees. *J. Hydrol.* 356 (1-2), 245-260.

548 Gaspar, L., 2011. Evaluación de la movilización y pérdida de suelo en agrosistemas de
549 secano mediante los radiotrazadores ^{137}Cs y $^{210}\text{Pb}_{\text{ex}}$. PhD Thesis, University of
550 Zaragoza. Spain, pp. 455.

551 Gaspar, L., Navas, A., Walling, D.E., Machín, J. y Gómez Arozamena, J., 2013. Using
552 ^{137}Cs and ^{210}Pb to assess soil redistribution on slopes at different temporal scales.
553 *Catena* 102, 46-54.

554 He, Q., Walling, D.E., 1996. Interpreting particle size effects in the absorption of ^{137}Cs
555 and unsupported ^{210}Pb by mineral soils and sediments. *J. Environ. Radioactiv.* 30, 117-
556 137.

557 Huh, C.-A., Su, C.-C., 2004. Distribution of fallout radionuclides (^7Be , ^{137}Cs , ^{210}Pb and
558 $^{239,240}\text{Pu}$) in soils of Taiwan. *J. Environ. Radioactiv.* 77 (1), 87-100.

559 Junge, B., Mabit, L., Dercon, G., Walling, D.E. Abaidoo, R., Chikoye, D., Stahr, K.,
560 2010. First use of the ^{137}Cs technique in Nigeria for estimating medium-term soil
561 redistribution rates on cultivated farmland. *Soil Till. Res.* 110, 211-220.

562 Kato, H., Onda, Y., Tanaka, Y., 2010. Using ^{137}Cs and $^{210}\text{Pb}_{\text{ex}}$ measurements to estimate
563 soil redistribution rates on semi-arid grassland in Mongolia. *Geomorphology* 114, 508-
564 519.

565 López-Vicente, M., Navas, A., 2010. Relating soil erosion and sediment yield to
566 geomorphic features and erosion processes at the catchment scale in the Spanish Pre-
567 Pyrenees. *Environ. Earth Sci.* 61, 143-158.

568 López-Vicente, M., Navas, A., Machín, J., 2008. Identifying erosive periods by using
569 RUSLE factors in mountain fields of the Central Spanish Pyrenees. *Hydrol. Earth Syst.*
570 *Sc.* 12 (2), 523-535.

571 Navas, A., Gaspar, L., Quijano, L., López-Vicente, M., Machín, J., 2012b. Patterns of
572 soil organic carbon and nitrogen in relation to soil movement under different land uses
573 in mountain fields (South Central Pyrenees). *Catena* 94, 43-52.

574 Navas, A., López-Vicente, M., Gaspar, L. y Machín, J. 2012a. Assessing soil
575 redistribution in a complex karst catchment using fallout ^{137}Cs and GIS.
576 *Geomorphology* doi:10.1016/j.geomorph.2012.03.018.

577 Navas, A., Valero-Garcés, B., Gaspar, L., Palazón, L., 2011. Radionuclides and stable
578 elements in the sediments of the Yesa Reservoir, Central Spanish Pyrenees. *J. Soils*
579 *Sediment.* 11, 1082-1098.

580 Navas, A., Walling, D.E., Gaspar, L., Machín, J., 2008. Use of Beryllium-7 to assess
581 soil redistribution by erosion in two contrasting Mediterranean environments. In:
582 *Sediment Dynamics in Changing Environments*. Schmidt, J., Cochrane, T., Phillips, C.,
583 Elliott, S., Davies, T., Basher, L. (Eds.) IAHS Publi. 325, pp. 43-51.

584 Porto, P., Walling, D.E., 2012. Validating the use of ^{137}Cs and $^{210}\text{Pb}_{\text{ex}}$ measurements to
585 estimate rates of soil loss from cultivated land in southern Italy. *J. Environ. Radioact.*
586 106, 47-57.

587 Porto, P., Walling, D.E., Callegari, G., Capra, A., 2009. Using caesium-137 and
588 unsupported lead-210 measurements to explore the relationship between sediment
589 mobilisation, sediment delivery and sediment yield for a Calabrian catchment. *Mar. and*
590 *Freshwater Res.* 60, 680-689.

591 Porto, P., Walling, D.E., Callegari, G., Catona, F., 2006. Using fallout lead-210
592 measurements to estimate soil erosion in three small catchments in southern Italy. *Water*
593 *Air Soil Pollut.* 6, 657-667.

594 Ritchie, J.C., McCarty, G.W., 2003. $^{137}\text{Cesium}$ and soil carbon in a small agricultural
595 watershed. *Soil Till. Res.* 69, 45-51.

596 Ritchie, J.C., McCarty, G.W., 2008. Redistribution of soil and soil organic carbon on
597 agricultural landscapes. In: Sediment Dynamics in Changing Environments. Schmidt, J.,
598 Cochrane, T., Phillips, C., Elliott, S., Davies, T., Basher, L. (Eds.) IAHS Publi. 325, pp.
599 135-138.

600 Sánchez-Cabeza, J.A., Garcia-Talavera, M., Costa, E., Peña, V., Garcia-Orellana, J.,
601 Nalda, C., 2007. Regional calibration of erosion radiotracers (^{210}Pb and ^{137}Cs):
602 Atmospheric fluxes to soils (N Spain). Environ. Sci. Technol. 41(4), 1324-1330.

603 Soto, J., Navas, A., 2004. A model of ^{137}Cs activity profile for soil erosion studies in
604 uncultivated soils of Mediterranean environments. J. Arid Environ. 59, 719-730.

605 Soto, J., Navas, A., 2008. A simple model of Cs-137 profile to estimate soil
606 redistribution in cultivated stony soils. Radiat. Meas. 43, 1285-1293.

607 Wakiyama, Y., Onda, Y., Mizugaki, S., Asai, H., Hiramatsu, S., 2010. Soil erosion rates
608 on forested mountain hillslopes estimated using ^{137}Cs and $^{210}\text{Pb}_{\text{ex}}$. Geoderma 159, 39-
609 52.

610 Wallbrink, P.J., Murray, A.S., 1993. The use of fallout radionuclide as indicators of
611 erosion processes. Hydrol. Process. 7, 297-304.

612 Walling, D.E., Collins, A.L., Sickingabula, H.M., 2003. Using unsupported lead-210
613 measurements to investigate soil erosion and sediment delivery in a small Zambian
614 catchment. Geomorphology 52, 193-213.

615 Walling, D.E., He, Q., 1999a. Using fallout lead-210 measurements to estimate soil
616 erosion on cultivated land. Soil Sci. Soc. Am. J. 63, 1404-1412.

617 Walling, D. E., He, Q., 1999b. Improved models for estimating soil erosion rates from
618 Cesium-137 measurements. J. Environ. Qual., 28, 611-622.

619 Walling, D.E., Quine, T.A., 1995. The use of fallout radionuclide in soil erosion
620 investigations. In: Nuclear Techniques in Soil-Plant Studies for Sustainable Agriculture

621 and Environmental Preservation. International Atomic Energy Agency Publication
622 ST1/PUB/947, 597-619.

623 Walling, D.E., Zhang, Y., He, Q., 2011. Models for deriving estimates of erosion and
624 deposition rates from fallout radionuclide (caesium-137, excess lead-210 and beryllium-
625 7) measurements and the development of user-friendly software for model
626 implementation. In: Impact of Soil Conservation Measures on Erosion Control and Soil
627 Quality. International Atomic Energy Agency Publication IAEA-TECDOC-1665, 11-
628 33.

629 Zhang, X., Qi, Y., Walling, D.E., He, X., Wen, A., Fu, J., 2006. A preliminary
630 assessment of the potential for using $^{210}\text{Pb}_{\text{ex}}$ measurement to estimate soil redistribution
631 rates on cultivated slopes in the Sichuan Hilly Basin of China. *Catena* 68, 1-9.

632 Zhang, X., Walling, D.E., Feng, M., Wen, A., 2003. $^{210}\text{Pb}_{\text{ex}}$ depth distribution in soil
633 and calibration models for assessment of soil erosion rates from $^{210}\text{Pb}_{\text{ex}}$ measurements.
634 *Chinese Sci. Bulletin* 48 (8), 813-818

635

636

637 **Tables**

638

639 Table 1. Basic statistics of $^{210}\text{Pb}_{\text{ex}}$ inventories (Bq m^{-2}), and the main physicochemical
 640 soil properties for cultivated and uncultivated soils. Different letters indicate significant
 641 differences at the p-level < 0.05 between cultivated and uncultivated soils.

642

643

| | Cultivated n=9 | | | | Uncultivated n=24 | | | |
|--|----------------|--------|--------|----------|-------------------|--------|--------|----------|
| | Min. | Max. | Mean | SD | Min. | Max. | Mean | SD |
| $^{210}\text{Pb}_{\text{ex}}$ Bq m^{-2} | b.d.l. | 7298.2 | 2975.9 | a 2904.4 | 325.7 | 5729.4 | 1933.2 | a 1042.4 |
| SOC % | 0.6 | 2.3 | 1.2 | a 0.6 | 1.0 | 10.1 | 4.6 | b 2.6 |
| Stoniness % | 5.0 | 55.9 | 27.0 | a 16.6 | 20.6 | 70.4 | 45.3 | b 12.6 |
| Clay % | 15.6 | 37.4 | 24.5 | a 6.1 | 11.9 | 40.8 | 23.4 | a 5.4 |
| Silt % | 35.7 | 77.6 | 63.5 | a 13.4 | 41.9 | 78.6 | 63.8 | a 8.6 |
| Sand % | 0.5 | 48.7 | 12.0 | a 16.4 | 0.1 | 46.2 | 12.8 | a 11.2 |

644 *SD standard deviation*645 *b.d.l. below detection limit*

646

647 Table 2. Mean values of $^{210}\text{Pb}_{\text{ex}}$ inventories (Bq m^{-2}) and the main physicochemical soil
 648 properties for different soil types in cultivated and uncultivated soils.

649

650

| | | Cultivated | | | Uncultivated | | |
|--|------|------------|----------|-----------|--------------|-----------|----------|
| | | Calcisols | Regosols | Gypsisols | Leptosols | Calcisols | Regosols |
| | | n=1 | n=4 | n=4 | n=3 | n=14 | n=7 |
| $^{210}\text{Pb}_{\text{ex}}$ Bq m^{-2} | Mean | 1654.6 | 1406.1 | 4876.0 | 1809.5 | 2056.2 | 1740.4 |
| | SD | - | 1837.0 | 3230.8 | 286.6 | 1208.5 | 942.2 |
| SOC % | Mean | 2.3 | 1.1 | 0.8 | 8.0 | 3.9 | 4.4 |
| | SD | - | 0.5 | 0.2 | 1.8 | 1.8 | 3.2 |
| Stoniness % | Mean | 48.8 | 33.1 | 15.2 | 53.9 | 41.7 | 49.0 |
| | SD | - | 16.7 | 7.7 | 2.9 | 12.5 | 13.7 |
| Clay % | Mean | 21.3 | 21.3 | 28.5 | 23.9 | 24.2 | 21.8 |
| | SD | - | 5.1 | 6.0 | 2.7 | 6.6 | 3.4 |
| Silt % | Mean | 49.9 | 64.4 | 66.1 | 67.1 | 60.3 | 69.2 |
| | SD | - | 19.5 | 5.1 | 2.5 | 7.7 | 9.2 |
| Sand % | Mean | 28.8 | 14.3 | 5.4 | 9.1 | 15.5 | 9.0 |
| | SD | - | 22.9 | 5.3 | 5.0 | 12.0 | 10.7 |

651 *SD standard deviation*

652

653 Table 3. Summary statistics of soil erosion and deposition rates (Mg ha⁻¹ year⁻¹) for
 654 sampling sites on cultivated and uncultivated soils.

655

| Mg ha ⁻¹ year ⁻¹ | n | Median | Mean | SD | SE | Min. | Max. | CV % |
|--|----|--------|------|------|------|------|-------|-------|
| Erosion | | | | | | | | |
| Cultivated | 5 | 12.9 | 32.1 | 35.4 | 15.8 | 4.2 | 83.7 | 110.3 |
| Uncultivated | 15 | 0.5 | 0.9 | 0.8 | 0.2 | 0.1 | 2.4 | 89.1 |
| Deposition | | | | | | | | |
| Cultivated | 4 | 56.5 | 54.1 | 20.6 | 10.3 | 28.6 | 74.75 | 38.1 |
| Uncultivated | 9 | 0.5 | 1.1 | 1.8 | 0.6 | 0.1 | 5.6 | 162.2 |

656 SD *standard deviation*

657 SE *standard error*

658

659 Table 4. Multiple range test for soil erosion and deposition rates ($\text{Mg ha}^{-1} \text{ year}^{-1}$)
 660 associated with different edaphic and physiographic characteristics. Different letters
 661 indicate significant differences at the p-level < 0.05 between different land uses, soil
 662 types and slope gradients, respectively.
 663

| | Erosion rate $\text{Mg ha}^{-1} \text{ year}^{-1}$ | | | Deposition rate $\text{Mg ha}^{-1} \text{ year}^{-1}$ | | |
|--------------|--|--------|------|---|--------|------|
| | n | Mean | SD | n | Mean | SD |
| Land use | | | | | | |
| Uncultivated | 15 | 0.9 a | 0.8 | 9 | 1.1 a | 1.8 |
| Cultivated | 5 | 32.1 b | 35.4 | 4 | 54.1 b | 20.6 |
| Soil type | | | | | | |
| Leptosols | 2 | 0.5 a | 0.3 | 1 | 0.1 a | - |
| Calcisols | 10 | 1.2 a | 1.6 | 5 | 1.5 a | 2.3 |
| Regosols | 7 | 10.9 a | 19.6 | 4 | 7.7 a | 13.9 |
| Gypsisols | 1 | 83.7 b | | 3 | 62.6 b | 14.3 |
| Slope % | | | | | | |
| 0-12 | 9 | 10.5 a | 27.5 | 6 | 37.2 b | 30.7 |
| 12-24 | 7 | 10.6 a | 19.8 | 5 | 0.3 a | 0.2 |
| > 24 | 4 | 1.1 a | 0.9 | 2 | 0.8 ab | 0.8 |

664 SD *standard deviation*

665

666 Table 5.a. Varimax rotated principal component loading (PCi) for the three first
 667 components (erosion rates). Loading factors higher than 0.5 (absolute value) are shown
 668 in bold.

669

| | PC1 | PC2 | PC3 | Estimated communality |
|--|-----------------|-----------------|-----------------|--------------------------|
| Use | 0.31186 | 0.83757 | 0.02315 | 0.79931 |
| Stoniness % | 0.18808 | -0.63599 | 0.18469 | 0.47397 |
| Erosion rates Mg ha ⁻¹ year ⁻¹ | -0.05773 | 0.86661 | -0.07046 | 0.75931 |
| Clay % | -0.75604 | 0.07373 | 0.02519 | 0.57767 |
| Silt % | -0.83205 | -0.03449 | -0.16506 | 0.72074 |
| Sand % | 0.97829 | -0.00531 | 0.11993 | 0.97147 |
| SOC % | 0.11328 | -0.66614 | -0.58696 | 0.80110 |
| Slope % | 0.20854 | -0.20802 | 0.83489 | 0.78381 |

670

671

672 Table 5.b. Varimax rotated principal component loading (PCi) for the two first
 673 components (deposition rates). Loading factors higher than 0.5 (absolute value) are
 674 shown in bold.

675

| | PC1 | PC2 | Estimated communality |
|---|-----------------|-----------------|--------------------------|
| Use | -0.91573 | 0.28580 | 0.92023 |
| Stoniness % | 0.81778 | -0.24505 | 0.72882 |
| Deposition rates Mg ha ⁻¹ year ⁻¹ | -0.92483 | 0.18565 | 0.88977 |
| Clay % | -0.37995 | 0.59488 | 0.49824 |
| Silt % | 0.06915 | 0.91820 | 0.84788 |
| Sand % | 0.12374 | -0.97653 | 0.96893 |
| SOC % | 0.61104 | -0.61082 | 0.74646 |
| Slope % | 0.77786 | 0.16928 | 0.63373 |

676

677

678 **Figures**

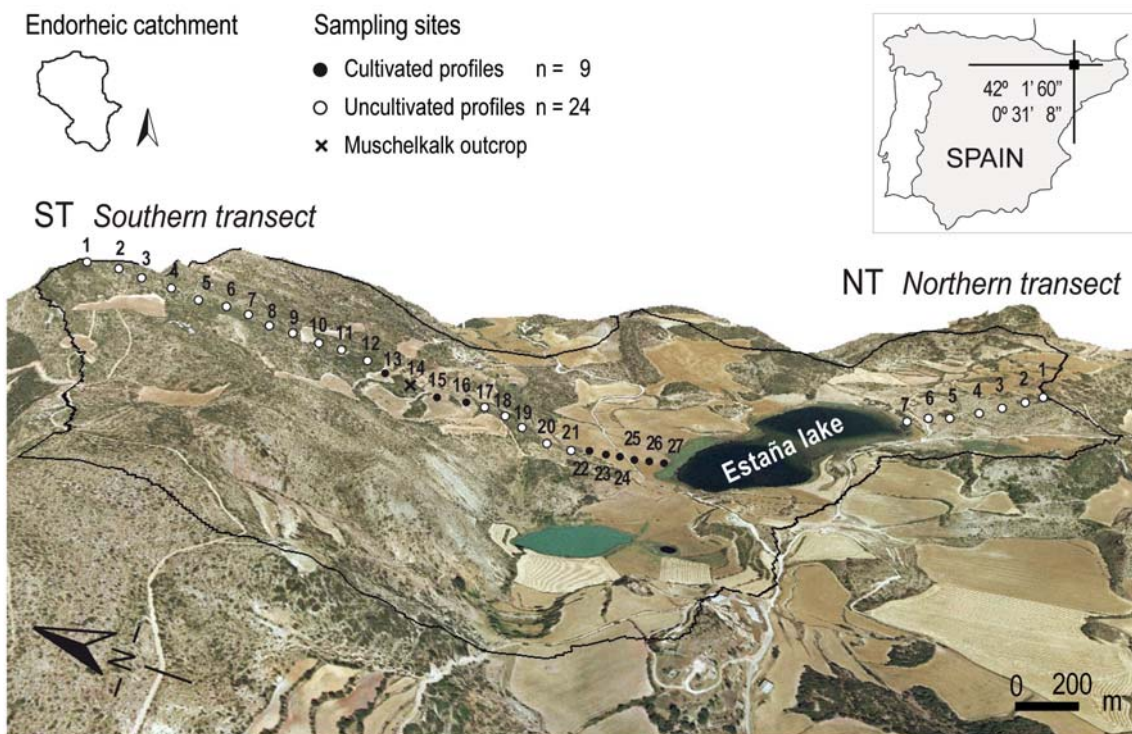
679

680 Figure 1. The study area located in the northern border of central part of the Ebro basin

681 (NE Spain) and the 34 sampling sites situated along southern (ST) and northern (NT)

682 transects.

683

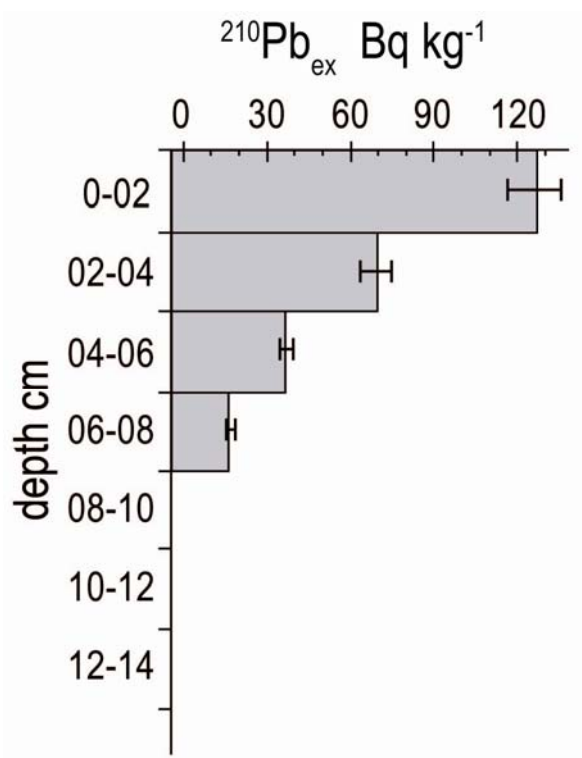


684

685

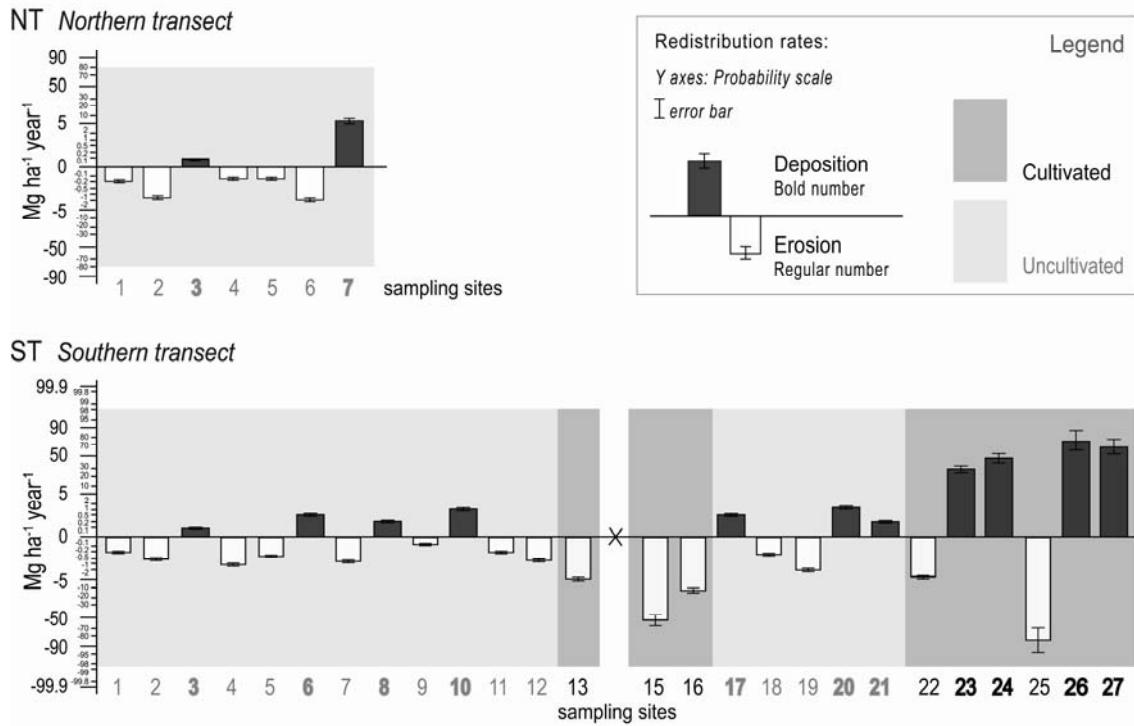
686 Figure 2. Representative depth distribution of $^{210}\text{Pb}_{\text{ex}}$ at the reference site.

687



688

689 Figure 3. Estimates of soil redistribution rates based on the $^{210}\text{Pb}_{\text{ex}}$ inventory
 690 measurements for the individual sampling points along northern (NT) and southern (ST)
 691 transect. Black numbers indicate cultivated soil profiles and grey numbers indicate
 692 uncultivated soil profiles.

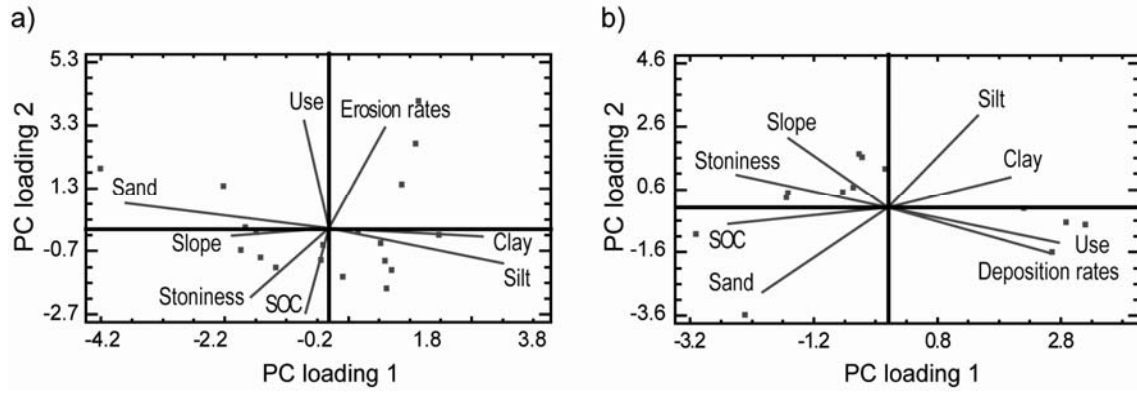


693

694

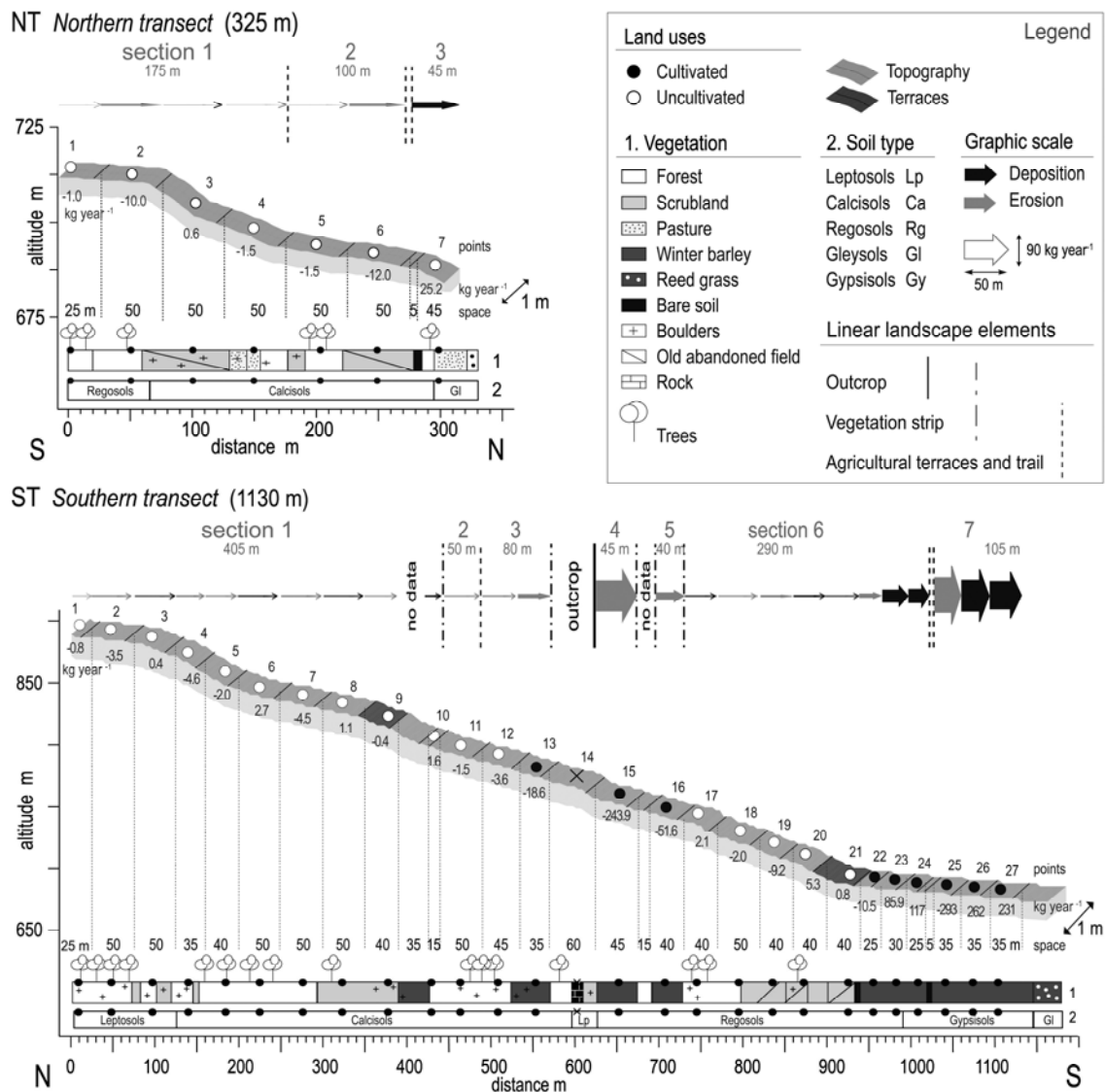
695 Figure 4. PCA biplot: dispersion diagram and principal components loadings, PC
696 loading 1 vs. PC loading 2 of cultivated and uncultivated soil samples after PCA
697 Varimax rotated for a) erosion rates and b) deposition rates.

698



699

700 Figure 5. Estimates of soil redistribution rates for individual slope segments and net soil
 701 loss along the northern (NT) and southern (ST) transects.



702